

Classification of Melanoma from Skin Lesion Images using Convolutional Neural Networks

Melvin Martin

Student, Dept of Biomedical Engineering, PSG College of Technology, Tamil Nadu, India

Abstract – Melanoma, a type of skin cancer is usually diagnosed by an autopsy, where a part of the suspicious skin area is taken and examined under laboratory conditions. To optimize and to reduce the time complexity involved in this process a deep learning model is trained and tuned to classify the dermoscopic images of skin lesions into eight different diagnostic categories.

Key Words: Classification, Skin cancer, CNN, Computer Vision, Screening.

1.INTRODUCTION

The unusual growth of cells in the skin layers often leads to skin cancer. Keratinocyte carcinoma and Melanoma are the most commonly occurring skin cancers. Keratinocyte carcinoma is also known as Non-melanoma skin cancer is most likely to occur on the head and neck as they are comparatively more exposed to UV rays. Melanoma, on the other hand, is caused by the outgrowth of benign moles formed by melanocytes. According to the world cancer research fund, Melanoma skin cancer ranks 19th in the most common cancer recorded globally [1].

The most useful application of computer vision in healthcare is to have faster and accurate predictions that would assess a clinician to have significant insights. The use of computer vision in classifying the skin lesion images into different cancer categories can be employed as a screening procedure.

2.DATASET

The dataset is obtained from the International Skin Imaging Collaboration (ISIC) containing dermoscopic images labeled into eight different categories as Actinic keratosis, Basal cell carcinoma, Squamous cell carcinoma, Melanoma, Melanocytic nevus, Benign keratosis, Dermatofibroma and Vascular lesion[2][3][4].

Actinic keratosis, a non-cancerous type found in red or pink patches in the skin. These patches may develop into squamous cell carcinoma if they are not treated. Basal cell carcinoma is the most common form affecting around 90% of the patients, they most likely to occur on the head or neck. Squamous cell carcinoma is grown as red, scaly lesions and is more aggressive than basal cell carcinoma, they are developed in the outer layers of skin. Melanoma, the rare and fatal type caused by pigment-creating cells called melanocytes. Melanocytic nevus is caused by the local

proliferation of melanocytes. They are benign and can be congenital or acquired. Benign keratosis, a non-cancerous skin lesion found as waxy, scaly, and slightly raised patches of skin. Dermatofibroma, a non-cancerous skin lesion more likely to occur in extremities and are common in immune-deficient individuals. Vascular lesion is a commonly occurring skin lesion also known as birthmarks. The class distribution of the dataset is shown in figure 1.

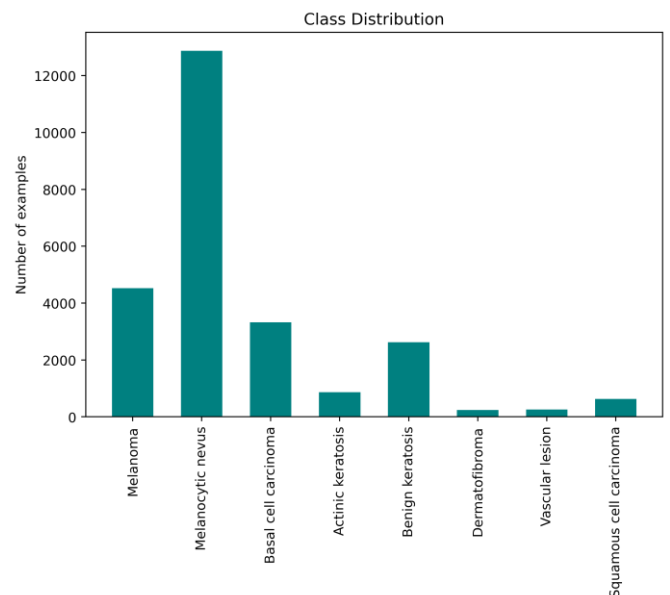


Fig-1: Class Distribution.

The dataset comprises 25,331 RGB images of size (600x450) and an excel sheet containing the image name and its corresponding label. The images for each class are shown in figure 2.

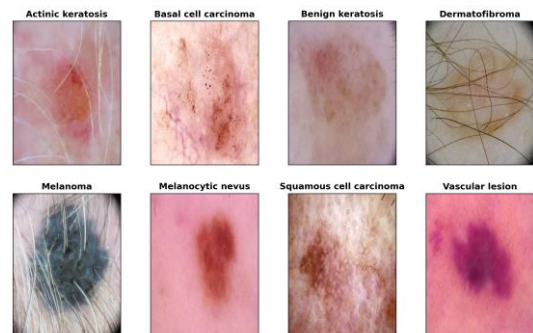


Fig-2: Sample images for each class.

3. DATA PREPROCESSING

The dataset mentioned in section 2 is preprocessed and separated according to their classes and kept in the folder hierarchy. The train-validation split ratio of the model is 80:20 where 20,269 images are used for training and 5,062 images for validation.

To address the class imbalance problem shown in figure 1, the images are augmented during training using the Keras class called ImageDataGenerator. The augmented images for each class and the augmentation operations are shown in figure 3 and table 1 respectively.

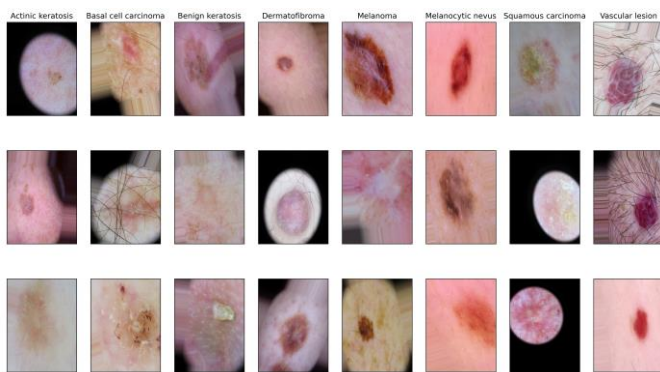


Fig-3: Sample augmented images for each class.

Operations	Range
Rescale	1/255.0
Roatation	20
Channel shift	0.2
Width shift	0.2
Height shift	0.2
Zoom	0.2
Shear	0.2
Horizontal flip	True
Fill mode	Nearest

Table-1: Augmentation operations.

4. MODEL ARCHITECTURE

To classify the skin lesion images various pre-trained models such as ResNet50, VGG16 and InceptionV3 are trained using the same loss, metrics, and validated based on the performance scores. As a result, ResNet50 outperforms the other architectures. The performance of the models is shown in figure 4.

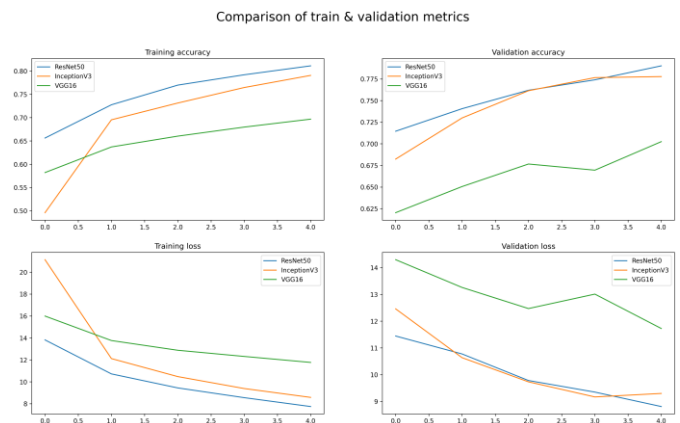


Fig-4: Performance comparison of different architectures.

To have a custom model architecture for classifying skin lesion images, the Global Average Pooling layer and a fully connected layer of 50 neurons are added to the resnet50 convolutional layers. Finally, a fully connected layer of 8 neurons is added to make the predictions corresponding to each class. The output weights are passed to the softmax activation function for the final predictions. The model architecture is shown in table 2.

Layers	Output shape	Number of parameters
Input Layer	(None, 600, 450, 3)	0
Resnet50	(None, 19, 15, 2048)	2,35,87,712
Global average pooling 2D	(None, 2048)	0
Dense 50 units	(None,50)	1,02,450
Dense 8 units (output layer)	(None,8)	408

Table-2: Model architecture.

5. MODEL TRAINING

To overcome the class imbalance problem shown in figure 1, the model is trained and experimented with three conditions

- 1.without image augmentation & categorical cross-entropy as loss function
- 2.with image augmentation & categorical cross-entropy as loss function
- 3.with image augmentation & custom loss function.

The custom loss function is a weighted version of categorical cross-entropy, ie the logits are multiplied by the weight w_i , where $w_i = k*(1 - \text{normalized class distribution})$. The equation of the custom loss function and the weights for each class is shown in equation 1 and table 3 respectively.

$$\text{Loss} = - \sum_{i=1}^{\text{number of classes}} w_i \cdot y_i \cdot \log \hat{y}_i \quad (1)$$

Class Names	Normalized class distribution	Weights (w _i)
Actinic keratosis	0.034	9.657
Basal cell carcinoma	0.131	8.688
Benign keratosis	0.103	8.963
Dermatofibroma	0.009	9.905
Melanoma	0.178	8.215
Melanocytic nevus	0.508	4.918
Squamous cell carcinoma	0.024	9.751
Vascular lesion	0.01	9.899

Table-3: Weights for loss function.

The model is trained using Adam optimizer with a learning rate of $1e^{-5}$ and validated using Precision and Recall. The model is experimented based on the above-mentioned conditions and the performance is illustrated in figure 5.

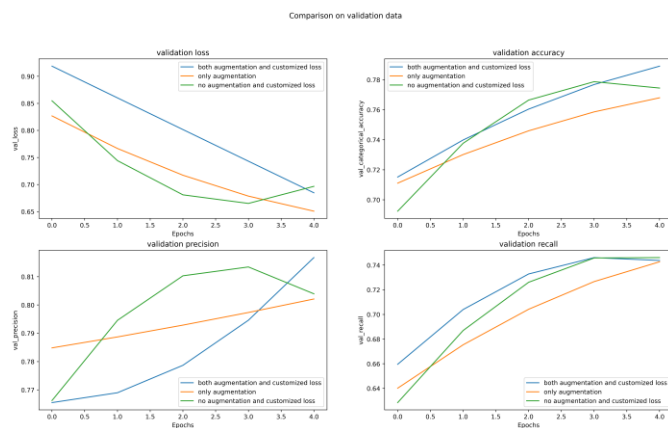


Fig-5: Comparison of metrics on validation data.

From figure 5 it is proven that using both image augmentation and weighted loss during training reduces overfitting and biased predictions on population dominant classes. As a result, the model is trained with image augmentation and weighted loss for another 15 epochs. The metrics at the end of training and training curves are shown in table 4 and figure 6 respectively.

Metrics	Train	Validation
Accuracy	0.967	0.828
Precision	0.963	0.831
Recall	0.955	0.817

Table-4 Metrics at the end of 20 epochs.

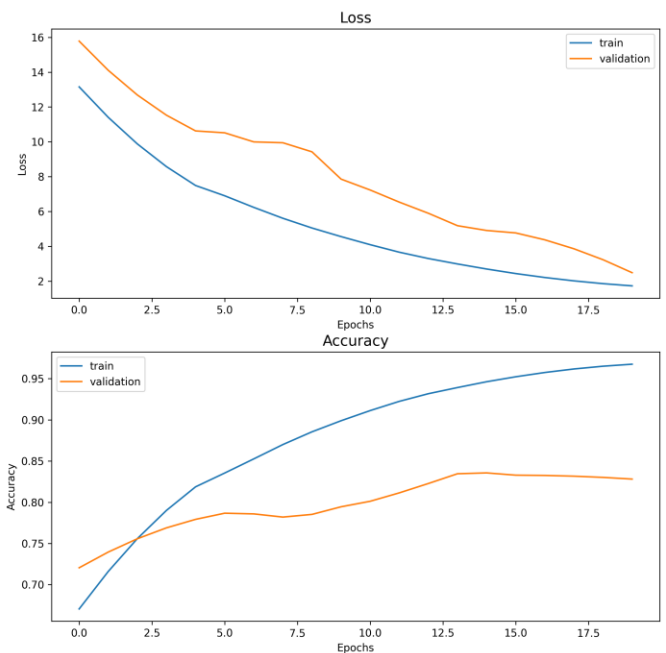


Fig-6: Training curves at the end of 20 epochs.

6. RESULTS

The proposed model pipeline eliminates biased predictions on sample dominant classes by prioritizing classes with a fewer number of examples during training. The confusion matrix and the metrics for each class are given in figure 7 and table 5 respectively.

In computer vision, visualizing the model's final activations can be helpful for stakeholders and decision-makers to check whether the model focuses on the key textures, patterns, or areas, this can be done using a technique called GradCam. It produces heatmaps also called Attention maps or class activation maps which highlights areas on which the model focuses. The activation map for each class is shown in figure 8.

		Confusion matrix								
Actual	AK	115	21	15	0	11	4	7	0	
	BCC	17	582	10	3	22	15	14	1	
	BKL	8	14	384	3	68	43	4	0	
	DF	2	5	0	34	1	5	0	0	
	MEL	15	18	16	0	738	114	3	0	
	NV	8	34	42	6	269	2209	0	7	
	SCC	11	12	5	4	10	2	81	0	
	VASC	0	0	0	0	1	0	0	49	
			AK	BCC	BKL	DF	MEL	NV	SCC	VASC
		Predicted								

Fig-7: Confusion matrix.

Classes	Precision	Recall	F1-score
Actinic keratosis	0.65	0.66	0.65
Basal cell	0.85	0.88	0.86

carcinoma			
Benign keratosis	0.81	0.73	0.77
Dermatofibroma	0.68	0.72	0.70
Melanoma	0.66	0.81	0.72
Melanocytic nevus	0.92	0.85	0.89
Squamous cell carcinoma	0.74	0.65	0.69
Vascular lesion	0.86	0.98	0.91

Table-5 Metrics for each class.

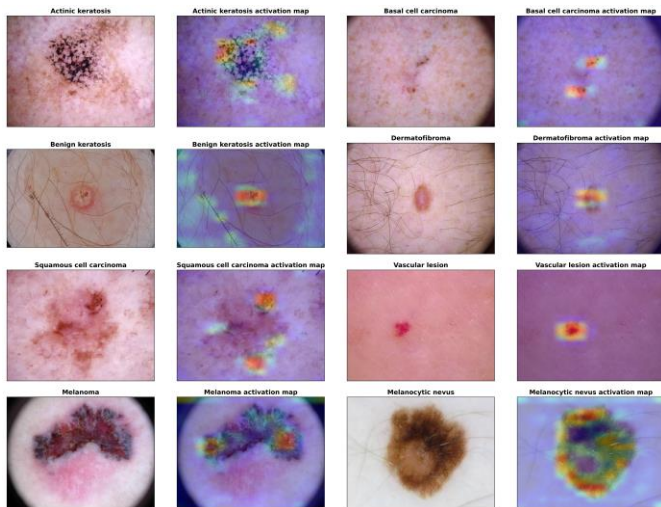


Fig -8: Class Activation maps.

A Machine learning model can only gain its value when the model's insights have routinely become accessible to users for which it is modeled, so it is important to deploy the model into production to derive clinical insights and monitor the model performance on real-time data. The model is deployed as both a web application and a mobile application.

The web application is developed using streamlit framework, an open-source python library for building custom web apps. The app file, model file, and the other required files are pushed into a GitHub repository and deployed in streamlit share. The URL for the web app is https://share.streamlit.io/melvin-martin/melanoma_classification/rps_app.py.

The mobile application is developed in Kotlin using Android Studio IDE. The model is quantized and optimized for size and latency and converted into the TensorFlow lite model, a suitable format for light-weighted devices. The mobile application has two pages, first one is a user interface for uploading the skin lesion image and obtaining the predictions, the second page is a user interface with web links that describes the class labels. The snapshots of web and mobile applications are shown in figures 9 and 10.

Fig -9: Mobile Application layout.

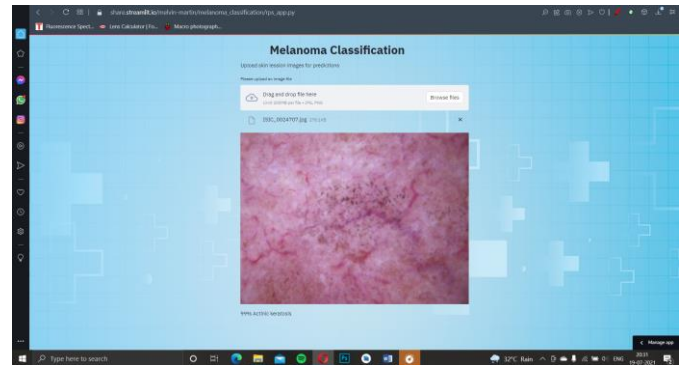


Fig -10: Web application.

7. CONCLUSION

In this paper, a convolutional neural network is designed and deployed to ease the diagnostic procedure and could be used as a screening tool for the early detection of skin cancer from skin lesion images. The performance of the model can be further improved by training on a larger class balanced dataset.

REFERENCES

- [1] <https://www.wcrf.org/dietandcancer/skin-cancer-statistics>
- [2] Tschandl P., Rosendahl C. & Kittler H. The HAM10000 dataset: a large collection of multi-source dermatoscopic images of common pigmented skin lesions. *Sci. Data* 5, 180161 doi:10.1038/sdata.2018.161 (2018)
- [3] Noel C. F. Codella, David Gutman, M. Emre Celebi, Brian Helba, Michael A. Marchetti, Stephen W. Dusza, Aadi Kalloo, Konstantinos Liopyris, Nabin Mishra, Harald Kittler, Allan Halber: "Skin Lesion Analysis Toward Melanoma Detection: A Challenge at the 2017 International Symposium on Biomedical Imaging (ISBI), Hosted by the International Skin Imaging Collaboration (ISIC)", 2017; arXiv:1710.05006.
- [4] Marc Combalia, Noel C. F. Codella, Veronica Rotemberg, Brian Helba, Veronica Vilaplana, Ofer Reiter, Allan C. Halber, Susana Puig, Josep Malvehy: "BCN20000: Dermoscopic Lesions in the Wild", 2019; arXiv:1908.02288.